Control system for a group of industrial mobile robots for moving large-sized objects

Dmitrii Shabanov[1], Nikolai Pirogov[2], Ayaulym Kuanyshova[1] and Valentin Kim[1]

[1] Peter the Great St.Petersburg Polytechnic University, 29, Polytechnicheskaya st., St.Petersburg, 195251, Russian Federation
[2] Chemnitz University of Technology, 62, Str. der Nationen, Chemnitz, 09111, Germany
dsb956@yandex.ru

Abstract. The article is devoted to the control system for a group of industrial wheeled mobile robots (WMR) for moving large-sized objects along a trajectory. The concept of a variable configuration transport cell (VCTC) consisting of a cargo and a group of WMRs is proposed. The formed transport cell belongs to the class of multi-wheeled vehicle. Dynamic control system which gives orders to WMRs in the form of force vectors is proposed. The dynamic control system allows to take into account additional cargo movement efficiency criteria. The VCTC mathematical model is developed. The inverse kinematics problem was solved and a feedback controller was proposed to be used in trajectory tracking controller. The research carried out in Simulink proved that the new concept can form the basis for a system, efficiently using drives. Efficiency can be achieved by the wheels slippage avoidance and by controlling the robots charge level during and after motion.

Keywords: wheeled mobile robot (WMR), trajectory tracking, variable configuration system, industrial transport system, multi-wheeled vehicle.

1 Introduction

This article deals with the industrial transport system based on the wheeled mobile robots (WMRs). The use of WMRs provides high flexibility and system's fault tolerance. A tractor robot with a trailer is the most flexible solution nowadays. However, such systems have the following disadvantages: cargo's weight limit, low efficiency at low-weight cargos transporting, and extremely low maneuverability. The implementation of "tractor-trailer robot" solution requires a difficult analysis of kinematics [1] and the development of a specific control system [2-4].

The proposed concept of a variable configuration transport cell (VCTC) allows to increase the transport system's flexibility and does not have the disadvantages mentioned above. The VCTC concept consists in moving the cargo by required number of single-type robots along a given trajectory.

The VCTC concept is partly based on the retractable football field [5], self-propelled modular transporter (SPMT) [6] (Fig. 1) and R. Stetter's industrial robot [7].

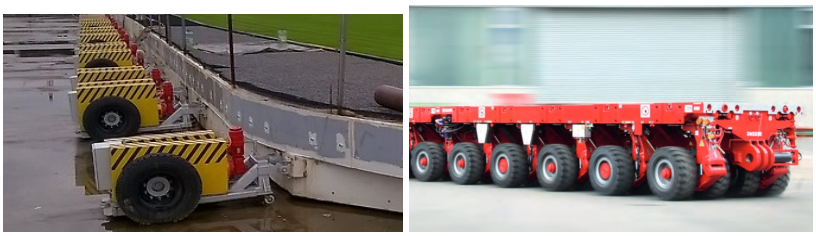

Fig. 1. Traction modules of the "Gazprom Arena" stadium and SCHEUERLE SPMT.

The SPMT and the retractable football field are considered to be a dynamic system due to providing load distribution between the drives/modules. The additional cargo movement efficiency criteria as the wheel slip avoidance or the robots charge level control are taken into account due to the dynamic approach. In such dynamic systems, the torque generated by motors should not affect the motion trajectory. The trajectory is set by a guide rail at the football field and by the wheels angle position at the SPMT.

2 Materials and methods

2.1 Variable Configuration Transport Cell

The Variable Configuration Transport Cell (VCTC) consists of a table, cargo and WMRs. Fig. 2 shows the VCTC kinematic diagram. The cargo is located on a table 1 with triple swivel casters 2. The differential drive WMRs 3 equipped with the coupling mechanisms 4 and the spring mechanisms 5 to ensure the drive wheels 6 traction with floor. The coupling mechanism allows the robots to turn to the desired angular position by creating the gearmotors' 7 velocity difference. The triple swivel casters 8 are required for robot's independent movement apart from the VCTC.

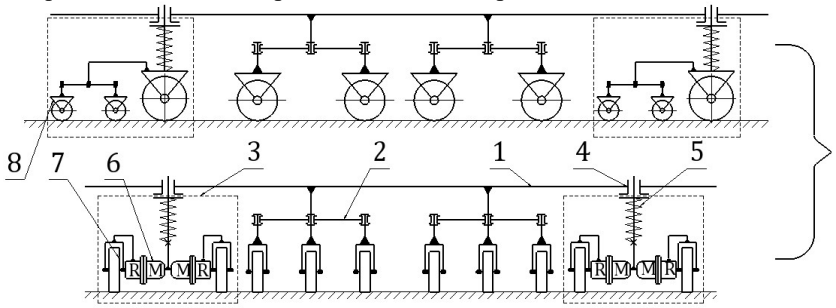

Fig. 2. Kinematic diagram of a Variable Configuration Transport Cell.

In case of a heavy-weight cargo, it can be advisable to replace the triple swivel casters with an air cushion [8]. In case of a low-weight cargo (which can be lifted by spring mechanisms), it is possible to replace triple swivel casters with support legs.

The VCTC configuration is defined as “variable”, because the WMRs number and docking places are determined by a cargo mass and a trajectory’s feature. The WMRs universality improves the industrial transport system's flexibility: same robots move cargos of any size and weight.

The proposed system allows complex motion performing. Robots take such positions to get each wheels' instant center of rotation (ICR) converged in one point. Fig. 3 shows the examples of possible transport cell motion and ICR positions.

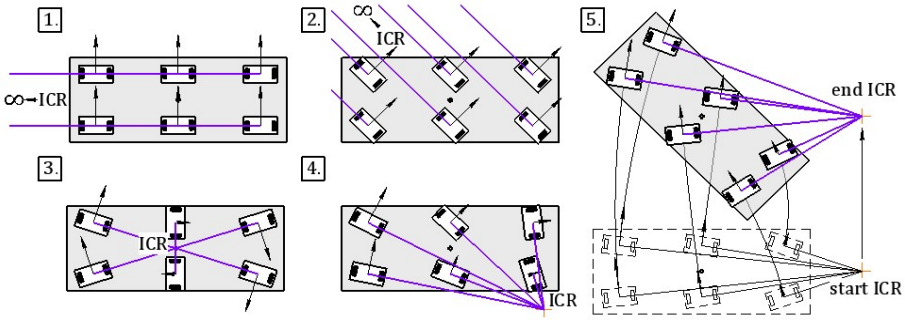

Fig. 3. Possible VCTC motions: linear motion (1, 2); rotation around its own center (3); rotation around adjusted center (4); complex motion with ICR movement (5)

2.2 Control system structure and dynamic approach

Fig. 4 shows the hierarchy of the transport system control based on hierarchy described in [9]. The VCTC control system solves only the Low-level control problems. High-level control is realized by a centralized intelligent industrial system. The centralized system selects robots for moving to a table, docking with it and forming the VCTC. Once the robot has finished the cargo's movement, it undocks and perform the following assigned tasks.

Consequently, the problem of VCTC is trajectory tracking. i.e. the VCTCs motion must comply with the law $\boldsymbol{q}^*(t) = [x^*(t), y^*(t), \varphi^*(t)]$.

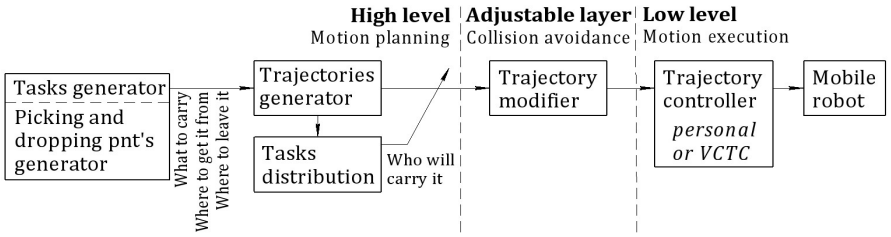

Fig. 4. Hierarchy of the transport system control

There are exist several basic approaches of trajectory tracking commonly based on: the robot's moving to a reference point or its motion at a reference velocity and direc-

tion, or the synthesis of both approaches [10-11]. If apply these approaches to the VCTC control, each of them will fully determine the WMRs reference values according to the law $\boldsymbol{q}^*(t)$, however the traction force generating by robots will not be controlled. This leads to uneven loading and wheels slipping, as well as uneven discharge of robots. It can lead to any of the robot's complete discharge before the motion ends.

Fig. 5 shows the VCTC control system's general structure. Proposed control system based on the dynamic approach implies giving an order to the WMRs in the form of the force vector $\boldsymbol{F}_i$. The power required to generate is determined from the law $\boldsymbol{q}^*(t)$ and can be obtained by various combinations of the $\boldsymbol{F}_i$ forces. Such variability allows to take into account additional criteria of VCTC motion efficiency.

The variability allows to use Torque Vectoring Strategy [12] and other methods of torque distribution (for example, [13]) for VCTC energy efficiency and slippage protection. An advanced risk assessment system [14] can be used to control the robot's charge level.

Moreover, it is important to have an optimal level of robot's charge after finishing cargo's movement. Robots may have an equal "middle" charge level sufficient to return to a charging station, but insufficient to complete the next task. Instead, it is possible to get half minimum charge level robots and half high-level charge robots to complete a next task.

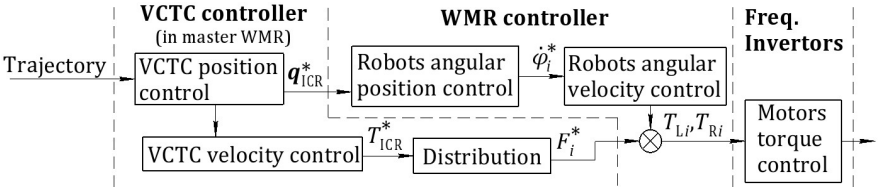

Fig. 5. VCTC control system's general structure.

The current positions and velocities of the robots and the VCTC are known via feedback sensors. The ICR desired position $\boldsymbol{q}_{ICR}$* fully determines the robots desired angular position. The "Distribution" part determines combination of robots forces $\boldsymbol{F}_i$ required to obtain $\boldsymbol{T}_{ICR}$*. The rolling resistance forces and inertial forces are not taken into account in the force $\boldsymbol{F}_i$* because they could be overcome by other robots' forces. Inertial characteristics are taken into account in m and I determination.

Only the "VCTC position control" and "VCTC velocity control" parts are considered in the article further. The WMR internal control system and the "Distribution" part were implemented to make experiments in Simulink.

2.3 Mathematical model

Fig. 6 shows a transport cell, which position is defined by the vector $\boldsymbol{q}(t) = [x(t), y(t), \varphi(t)]$. The variables x and y indicate the center mass C position in a global coordinate system in the movement plane. The current position $\boldsymbol{q}(t)$ is calculated using the robot's feedback sensors output values.

VCTC-fixed coordinate system m is centered at the C point. The angular position φ is defined as the angle between X_m and X axes. The WMRs (2) move the cargo using

joints formed by coupling mechanisms (3) with the F_i force at the φ_i angle. The joints are located at $[x_{mi}, y_{mi}]$ in the m coordinate system. The equivalent mass m and equivalent moment of inertia I are determined from the VCTC mass characteristics and the rotors inertia.

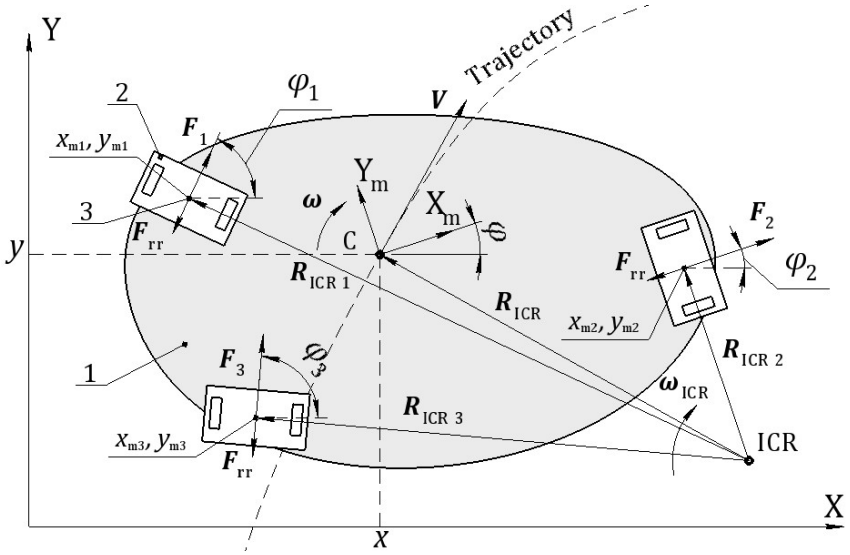

Fig. 6. Mathematical model.

The following values are shown on Fig. 6:
$\boldsymbol{V}$ – the VCTC line velocity;
ω – the VCTC angular velocity relative to the center of mass;
$\boldsymbol{F}_{rr}$ – the robot's equivalent wheel rolling resistance force;
$\boldsymbol{q}_{ICR} = [\boldsymbol{x}_{ICR}, \boldsymbol{y}_{ICR}]$ – the position of the instant center of rotation (ICR);
$\boldsymbol{R}_{ICR}$ – the distance between the VCTC center of mass and the ICR;
$\boldsymbol{R}_{ICRi}$ – the i robot's lever arm relative to the ICR;
ω_{ICR} – VCTC rotation velocity relative to the ICR (numerically equal to ω_{VCTC});
I_{ICR} – the equivalent moment of inertia of the VCTC relative to the ICR.

The weight is assumed to be evenly distributed over the robots' wheels. This assumption allows to simplify the rolling resistance force calculation and at the same time does not affect the control system design and experiments conduction in the Simulink.

The VCTC linear motion kinetic energy can flow into rotational kinetic energy and back during robot's rotation i.e., while the ICR change. Therefore, linear and angular velocities are calculated from kinetic energy. The kinetic energy can be calculated as the integral of the powers developing by the traction and rolling resistance forces. Performing calculations relative to the ICR make possible to represent complex motion as rotational motion:

$$E_k(t) = \int_0^t \sum_{i=1}^{n} (\boldsymbol{F}_i(t) \times \boldsymbol{R}_{ICRi}(t) \cdot \omega_{ICR}(t) - F_{rr} \cdot R_{ICRi}(t) \cdot \boldsymbol{\omega}_{ICR}(t)) dt \qquad (1)$$

Lever arms are better to calculate in matrix form:

$$\boldsymbol{R}_{\mathrm{ICR}i}(t)=\begin{bmatrix}x_{\mathrm{m}i} & y_{\mathrm{m}i}\end{bmatrix}\begin{bmatrix}\cos(\varphi(t)) & \sin(\varphi(t))\\ -\sin(\varphi(t)) & \cos(\varphi(t))\end{bmatrix}+\begin{bmatrix}x(t) & y(t)\end{bmatrix}-\boldsymbol{q}_{\mathrm{ICR}}(t) \tag{2}$$

As the motion was represented as rotation around the ICR it is possible to calculate the VCTC's ω_{ICR} and ω angular velocities, linear velocity V and position $\boldsymbol{q}$.

$$E_{\mathrm{k}}(t)=\frac{mV^2(t)}{2}+\frac{I\omega^2(t)}{2}=\frac{I_{\mathrm{ICR}}(t)\omega_{\mathrm{ICR}}^2(t)}{2} \tag{3}$$

$$I_{\mathrm{ICR}}(t)=I+m\cdot R_{\mathrm{ICR}}^2(t) \tag{4}$$

$$\boldsymbol{R}_{\mathrm{ICR}}(t)=\begin{bmatrix}x(t) & y(t)\end{bmatrix}-\boldsymbol{q}_{\mathrm{ICR}}(t) \tag{5}$$

$$\omega(t)=\omega_{\mathrm{ICR}}(t)=\left(\frac{2E_{\mathrm{k}}(t)}{I_{\mathrm{ICR}}(t)}\right)^{0.5} \tag{6}$$

$$\boldsymbol{V}(t)=\boldsymbol{\omega}(t)\times\boldsymbol{R}_{\mathrm{ICR}}(t) \tag{7}$$

$$\varphi(t)=\int_0^t\omega(t)dt\,;\,x(t)=\int_0^t V_{\mathrm{X}}(t)dt\,;\,y(t)=\int_0^t V_{\mathrm{Y}}(t)dt \tag{8}$$

2.4 Trajectory tracking control

Inverse kinematics-based method (IK-method). At any instant of time t, there is a value $\tau(t)$ that $\boldsymbol{q}^*(\tau(t))$ is the closest point to $\boldsymbol{q}(t)$ located on the trajectory (Fig. 7). In case the VCTC follows the trajectory precisely then $\tau(t)=t$. The $\boldsymbol{q}^*(\tau(t)+dt)$ and $\boldsymbol{q}^*(\tau(t)+2dt)$ are the desired VCTC positions during the dt and $2dt$ times accordingly. The ICR desired position is calculated from linear and angular velocities ratio. The velocities are calculated as the ratio of distance between $\boldsymbol{q}^*(\tau(t)+dt)$ and $\boldsymbol{q}(t)$ to the time.

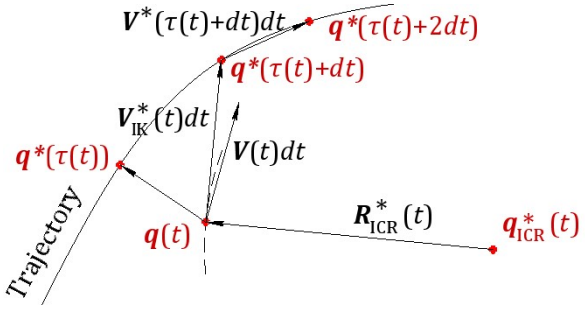

Fig. 7. Vectors used in the IK-method.

$$\dot{\boldsymbol{q}}_{\mathrm{IK}}^*(t)=\frac{\boldsymbol{q}^*(\tau(t)+dt)-\boldsymbol{q}(t)}{dt}=\left[V_{\mathrm{IK\,X}}^*(t),V_{\mathrm{IK\,Y}}^*(t),\omega_{\mathrm{IK}}^*(t)\right] \tag{9}$$

$$\boldsymbol{R}_{\mathrm{ICR}}^*(t)=\frac{\boldsymbol{V}_{\mathrm{IK}}^*(t)}{\omega_{\mathrm{IK}}^*(t)}\cdot\begin{bmatrix}\cos(\pi/2) & -\sin(\pi/2)\\ \sin(\pi/2) & \cos(\pi/2)\end{bmatrix} \tag{10}$$

$$\boldsymbol{q}^*_{\mathrm{ICR}}(t) = \begin{bmatrix} x(t) & y(t) \end{bmatrix} - \boldsymbol{R}^*_{\mathrm{ICR}}(t) \tag{11}$$

The desired torque T_{ICR}*(t) can be calculated in the same way. The current value of kinetic energy $E_{\mathrm{k}}(t)$ can be calculated from the VCTC's current velocities. It is possible to calculate the required kinetic energy E_{k}*($\tau(t)+dt$) by the difference between states $\boldsymbol{q}$*($\tau(t)+dt$) and $\boldsymbol{q}$*($\tau(t)+2dt$):

$$\dot{\boldsymbol{q}}^*(\tau(t)+dt) = \frac{\boldsymbol{q}^*(\tau(t)+2dt) - \boldsymbol{q}^*(\tau(t)+dt)}{dt} = \\ = \left[V^*_{\mathrm{X}}(\tau(t)+dt), V^*_{\mathrm{Y}}(\tau(t)+dt), \omega^*(\tau(t)+dt) \right] \tag{12}$$

$$E^*_{\mathrm{k}}(\tau(t)+dt) = \frac{mV^{*2}(\tau(t)+dt)}{2} + \frac{I\omega^{*2}(\tau(t)+dt)}{2} \tag{13}$$

$$\Delta E_{\mathrm{k}} = T_{\mathrm{ICR}} \cdot \omega_{\mathrm{ICR}} \cdot \Delta t \Rightarrow T^*_{\mathrm{ICR}}(t) = \frac{E^*_{\mathrm{k}}(\tau(t)+dt) - E_{\mathrm{k}}(t)}{\omega(t) \cdot dt} \tag{14}$$

Torque controller. The IK-method eliminates deviations from the trajectory but can't eliminate the $\boldsymbol{t-\tau(t)}$ error. The value $\boldsymbol{t-\tau(t)}$ and the torque $\boldsymbol{T_{ICR}}$*$\boldsymbol{(t)}$ are related by second-order differential equation. Therefore, for the error elimination a two-circuit controller with kinetic energy control is needed. For the system's correct work at the low $\boldsymbol{R_{ICR}(t)}$ and at the infinitely large one, the controller's output multiplies by $\boldsymbol{R_{ICR}(t)}$. Fig. 8 shows the torque controller and mathematically it is described as follows**:**

$$T^*_{\mathrm{ICR}}(t) = \mathrm{PID}(E^*_{\mathrm{k}}(\tau(t)+dt) - E_{\mathrm{k}}(t) + \mathrm{PID}(t-\tau(t))) \cdot R^*_{\mathrm{ICR}}(t) \tag{15}$$

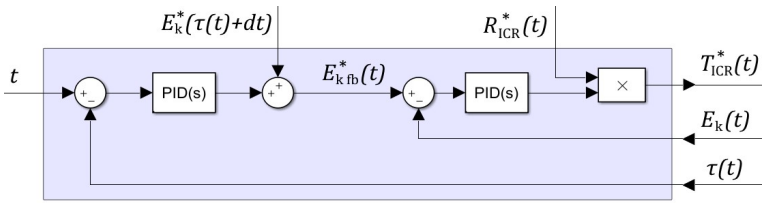

Fig. 8. Torque controller.

The way of VCTC's entering the trajectory also impacts on a t-$\tau(t)$ error. The described controller will move the VCTC to the trajectory's nearest point. Then VCTC will make a sharp turn and start moving along the trajectory. It is possible to enter the trajectory smoothly by tangential as an alternative option. Fig. 11 shows a simulation results of both ways of trajectory entering. For a smooth trajectory entering it is required to replace $\tau(t)$ with t in the IK-method.

Smooth trajectory entering may lead to a collision with another object located near the trajectory. Moving to the nearest trajectory point can result in high accelerations occurrence during sharp turn. Smooth trajectory entering provides a significantly less t-$\tau(t)$ error.

Feedback control method. The IK-method can be modified to get some problems solved. For example, the trajectory tracking control's stiffness can be reduced to in-

crease smooth motion. Moreover, modified controller can form the basis for a collision avoidance controller. It is proposed to use a feedback controller with a structure similar to the inverse model.

The initial values $q_{ICRst}^*(t)$ and $E_{k\,st}^*(t)$ are calculated by the equations (9,10,12,13) with replacing $q(t)$ by $q^*(\tau(t))$. The current VCTC position error can be calculated as the difference between the desired and current positions: $q_e(t) = q^*(\tau(t))- q(t) = [x_e(t), y_e(t), \varphi_e(t)]$. The linear error consists of the component $q_{eC}(t)$ collinear to $R_{ICRst}^*(t)$ and the component $q_{eP}(t)$ perpendicular to $R_{ICRst}^*(t)$ (Fig. 9). The initial reference values changes according to the technology presented in the in Table 1 to eliminate the errors.

Table 1. Errors elimination technology.

Error	Way to eliminate the error	Controller
$\varphi_e(t)$	Increase or decrease of the distance to the ICR	$R_{ICR}^*(t)= R_{ICRst}^*(t)(1\text{-PID}(\varphi_e(t)))$
$q_{eC}(t)$	Moving the ICR along an arc by the angle α	$\alpha(t)=\text{PID}(q_{eC}(t))$
$q_{eP}(t)$ $t - \tau(t)$	Change of kinetic energy by torque	$E_{k\,fb}^*(t)= E_{k\,st}^*(t)+\text{PID}(q_{eP}(t))+\text{PID}(t - \tau(t))$

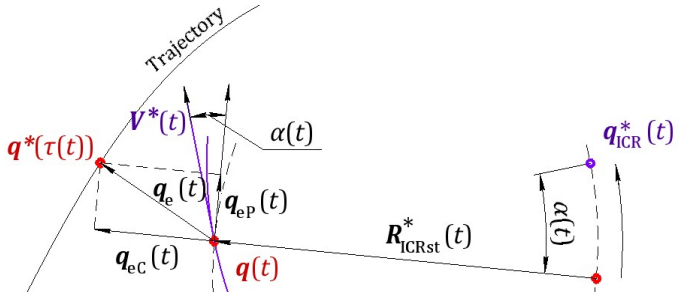

Fig. 9. Components of $\boldsymbol{q}_e(t)$ errors and ICR rotation.

Moving the ICR along an arc by the angle α rotates the linear velocity vector at the same angle (Fig. 9). The desired position of ICR is calculated as follows:

$$\boldsymbol{q}_{ICR}^*(t) = \begin{bmatrix} x(t) & y(t) \end{bmatrix} - \boldsymbol{R}_{ICR}^*(t) \tag{16}$$

$$\boldsymbol{R}_{ICR}^*(t) = \boldsymbol{R}_{ICRst}^*(t) \cdot \begin{bmatrix} \cos(\alpha(t)) & -\sin(\alpha(t)) \\ \sin(\alpha(t)) & \cos(\alpha(t)) \end{bmatrix} \cdot \left(1 - \text{PID}(\varphi_e(t))\right) \tag{17}$$

3 Results

The proposed system was simulated in Simulink environment. The VCTC has the following parameters:

– equivalent mass m=1000 kg;
– equivalent moment of inertia I=450 kg·m^2;
– amount of traction robots – 4 pc.;
– one robot's maximum traction force F_{max}=130 N;

Robots' positions are shown in Fig. 10. The trajectory was set by a Bezier curve to exclude instant velocity changes. The curve is divided into three sections (Fig. **11**): in section I the transport cell rotates with an angular velocity π/12 rad/s; in section II the cell's rotation smoothly decelerates; in section III the transport cell maintains an angular position of 1.5 π rad. Transport cell's initial deviation is [2 0.5] (m). Linear speed of motion: 1m/s.

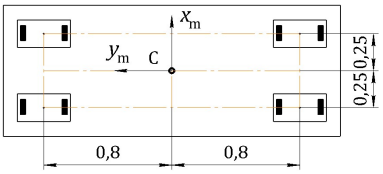

Fig. 10. Robots positions.

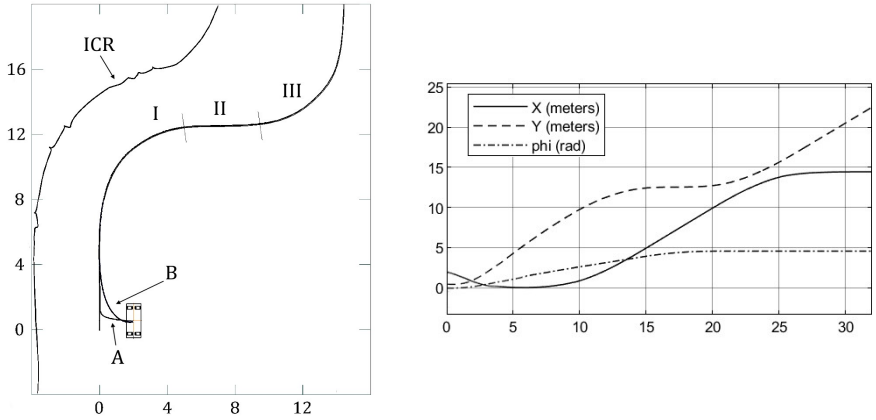

Fig. 11. Transport cell's motion.

The simulation results are shown in Fig. 11 and Fig. 12. The IK-method and feedback controller's graphs are look similar. Therefore, the IK-method's graphs only are shown.

The letter A on the graphs shows a cell's motion with a sharp trajectory entering without t-$\tau(t)$ delay control; the letter B shows a cell's motion with a smooth trajectory entering with a t-$\tau(t)$ delay control. The ICR motion trajectory also shown on Fig. 11. The maximal deviations after entering the trajectory are shown in Table 2.

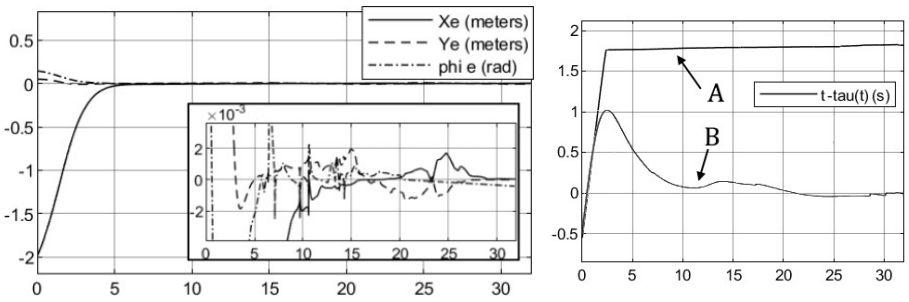

Fig. 12. q_e and t - $\tau(t)$ errors.

Table 2. Maximal errors $q_{e.}$

Control method	x_e ,m	y_e ,m	φ_e ,rad
IK-method	$2 \cdot 10^{-2}$	$1 \cdot 10^{-2}$	$1.6 \cdot 10^{-2}$
Feedback controller	$6 \cdot 10^{-2}$	$4 \cdot 10^{-2}$	$8 \cdot 10^{-2}$

4 Discussion

The obtained results show the possibility of using the ICR position and the total torque relative to ICR as the WMR's reference values. The obtained error values show the upper bound of the system accuracy. The system's accuracy level e (maximal deviations from the trajectory) on a straight trajectory with further turn along the radius R with the velocity V can be evaluated by the ratio:

$$e = k \cdot V / R, \tag{18}$$

Where coefficient k=0.5 m·s is found from the experiment with parameters V=1m/s and R=7m. The found error value is e=7.2·10^{-2}m.

The robot's angular position control system has a significant impact on the accuracy. Therefore, it is necessary to use highly effective robot's angular position controlling methods such as reinforcement learning [15].

It is mathematically possible to convert the IK-method to the feedback controller form. It allows to estimate the controller coefficients optimal values. However, some of the values will be related with variables (e.g. velocities). This demonstrates the potential efficiency of open-loop adaptive controller [16] use in solving the VCTC motion problem.

5 Conclusion

The variable configuration transport cell (VCTC) advantages were shown in comparison with traditional WMR-based industrial transport systems.

To carry out the experiments in Simulink the VCTC's mathematical model was developed. The results show the dynamic approach's ability to solve the VCTC motion

problem. The dynamic approach implies giving orders to the mobile robots in the form of desired angular positions and desired traction forces values. It allows to distribute tractive force between robots without affecting velocity and direction of motion. This distribution can provide the drives efficient use by taking into account a number of additional criteria, such as:

- no wheel slippage
- providing robot's desired charge level after the motion's end
- providing robot's required charge level during the motion.

The simulation results show a high accuracy of a given trajectories following by the proposed system.

References

1. Michalek, M.: Trailer-Maneuverability in N-Trailer Structures. IEEE Robotics and Automation Letters, 5(4), 5105-5112 (2020).
2. Ritzen, P. et al: Trailer Steering Control of a Tractor–Trailer Robot. IEEE Transactions on Control Systems Technology, 24(4), 1240-1252 (2015).
3. Binh, N.T. et al: An Adaptive Backstepping Trajectory Tracking Control of a Tractor Trailer Wheeled Mobile Robot. Int. J. of Control, Automation, and Systems, 17, 465–473 (2019).
4. Kassaeiyan, P. et al: Control of tractor-trailer wheeled robots considering self-collision effect and actuator saturation limitations. Mechanical Systems and Signal Processing, 127, 388–411 (2019).
5. Volkov, A.N. et al: Retractable football field for indoor stadium. Patent Russian Federation no. RU 161988 U1 (2016).
6. Lavrikov, A.A. et al: Control of Movement of a Loosely Coupled Self-Propelled Modular Transporter. J. of Machinery Manufacture and Reliabilit, 48(1), 20-25 (2019).
7. Stetter, R., Ziemniak, P. et al: Development, Realization and Control of a Mobile Robot. In: Obdržálek, D., Gottscheber, A. (eds.) Int. Conf. on Research and Education in Robotics – EUROBOT 2010, 130-140, Springer, Heidelberg (2011).
8. Kochneva, O.V. et al: Mobile robotic air cushion system. In: IOP Conf. Ser.: Earth and Environmental Science, 539, 012119 (2020).
9. Adinandra, S., Kosti´c, D. et al.: Towards a Flexible Transportation in Distribution Centers - Low-level Motion Control Approach. In: Proceedings of the 8th Int. Conf. on Informatics in Control, Automation and Robotics, 2, 155-160. SciTePress, Setúbal (2011).
10. Klanˇcar, G., Zdešar, A., Blaži ˇc, S. et al: Wheeled Mobile Robotics. 1st edn. Butterworth-Heinemann, Kidlington (2017).
11. Corke, P.: Robotics, Vision and Control. Fundamental Algorithms in MATLAB. 1st edn. Springer, Heidelberg (2011).
12. Ghosh, J., Tonoli, A. et al: A Torque Vectoring Strategy for Improving the Performance of a Rear Wheel Drive Electric Vehicle. In: 2015 IEEE Vehicle Power and Propulsion Conf., IEEE, Montreal (2015).
13. Park, J. et al: Torque Distribution Algorithm for an Independently Driven Electric Vehicle Using a Fuzzy Control Method. Energies, 8(8), 8537-8561 (2015).
14. Berenz, V. et al.: Autonomous battery management for mobile robots based on risk and gain assessment. Artificial Intelligence Review, 37(3), 217–237 (2012).

15. Dziomin, U. et al: A Multi-Agent Reinforcement Learning Approach for the Efficient Control of Mobile Robot. In: The 7th IEEE Int. Conf. on Intelligent Data Acquisition and Advanced Computing Systems: Technology and Applications, 867-873, IEEE, Berlin (2013).
16. Landau, I.D. et al: Adaptive Control. Algorithms, Analysis and Applications. 2nd edn. Springer, London (2011).